Synergic green technologies for treatment of hexavalent chromium polluted waters
Project PNII-RU-TE-2014-4-0508
No. 129/1/10/2015

Scientific report

Phase 1: 01.10.2015 – 31.12.2015

Objective 1. Ensuring the necessary conditions for the research activities
Activities: The needed existent materials have been identified and prepared. Other needed, but not existent, materials have been purchased (chemical reagents: Fe^0, MnO_2). The analytical methods have been selected and prepared in order to support the research activities.

Objective 2. Investigation of the effect of sand co-presence on Cr(VI) removal with Fe^0
Activities: Batch treatability experiments for Cr(VI) removal with Fe0 in the co-presence of sand.

2.1. Materials and methods

Commercially available Fe^0 (≥ 99%, ~10 μm) from Merck was used in this assay as received. Sand obtained from a local source was sieved to obtain the following grain sizes: 0.1-0.5 mm, 0.5-1.25 mm, 1.25-2 mm and 2-5 mm; the sand was then washed with distilled water and dried. Cr(VI) stock solutions (10 g/L) were prepared by dissolving 28.29 g $K_2Cr_2O_7$ in 1000 mL of distilled deionized water. Working solutions of the desired initial Cr(VI) concentration (2 mg/L) were prepared by diluting the stock solution. Experiments were conducted in a 1.5 L Berzelius flask open to the atmosphere, containing 1000 mL of Cr(VI) working solution. The reactive solids were added to the Cr(VI) solution and the flask content was mixed continuously by a Heidolph vertical agitator equipped with a polymethacrylate stirring shaft. Initial Cr(VI) concentration (2 mg/L), working volume (1000 mL), solution pH (2.5), mixing rate (200 rpm) and temperature (22 ^oC) were held constant throughout the study. The pH was adjusted to 2.5 by small addition of concentrated H_2SO_4 and measured in samples collected before and after the reaction using an Inolab pH-meter. pH 2.5 was selected because it was previously reported that experiments of Cr(VI) removal with Fe^0 in batch system can be best carried out in an acidic environment (Gheju and Iovi, 2006). Additional experiments were conducted at 6 and 32 ^oC in order to study the influence of temperature, keeping all other conditions equal. Samples were collected at predetermined time intervals, filtered and analyzed. Chromium and iron dissolved species were determined by colorimetric methods, using a Jasco V 530 spectrophotometer. Chromium and iron dissolved species were determined by colorimetric methods, using a Jasco V 530 spectrophotometer (Standard Methods, 1995). Cr(VI) concentration was determined by the 1,5-diphenylcarbazide method, at 540 nm. Cr(total) was analyzed by oxidizing any Cr(III) with potassium permanganate, followed by analysis as Cr(VI). Cr(III) was determined from the difference between Cr(total) and Cr(VI). Fe(II) concentrations were determined by the 1,10-ortophenanthroline method, at 510 nm; Fe(total) was determined by reduction of any Fe(III) to Fe(II) with hydroxylamine hydrochloride followed by analysis as Fe(II). Fe(III) was determined from the difference between total and bivalent iron. The calibration curves of Cr(VI) and Fe(II) are depicted in Fig.1 and 2.

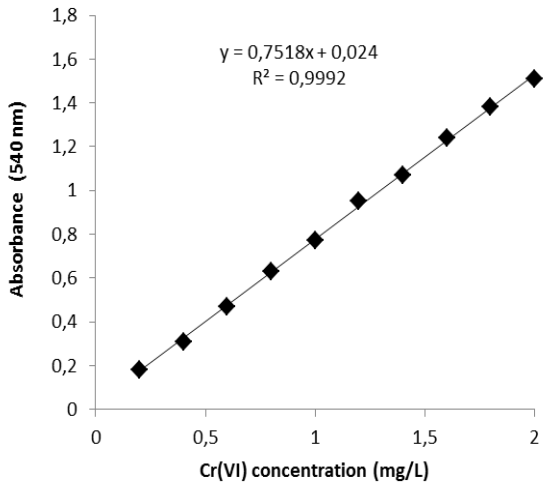

Fig.1. Cr(VI) calibration curve

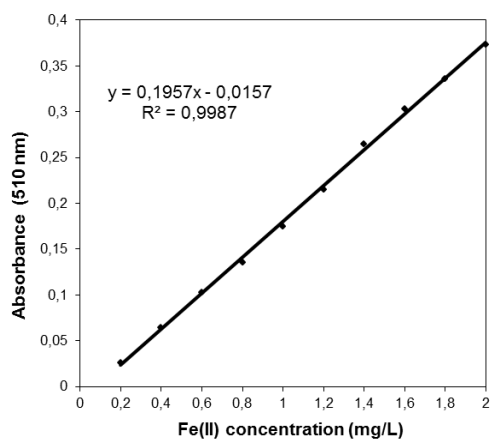

Fig.2. Fe(II) calibration curve

The point of zero charge (pH_{pzc} - the pH at which the net surface charge takes a zero value) was determined using the pH drift method, by contacting the solid samples with 0.01 M NaCl solutions at various pH (1–10), and allowing to equilibrate for 24 h in a shaking bath. Then the final pH value of the supernatant for each initial pH was measured. The pH_{PZC} was determined graphically at the intersection of the curve $pH_{fin} = f(pH_{in})$ with the line $pH_{fin} = pH_{in}$ (Zach-Maor et al., 2011).

2.2. Results and discussion

2.2.1. Removal of Cr(VI) in H_2O-Fe^0-Cr(VI) system

Even though numerous studies have investigated the Cr(VI) removal in H_2O-Fe^0-Cr(VI) system, there is still some controversy in what concerns the mechanism and kinetics of the process.

Therefore, in this study we have also examined the removal of Cr(VI) with bare Fe^0 (no sand or MnO_2), at two doses, 0.5 and 1.0 g/L; the results are presented in Figs. 3 and 4.

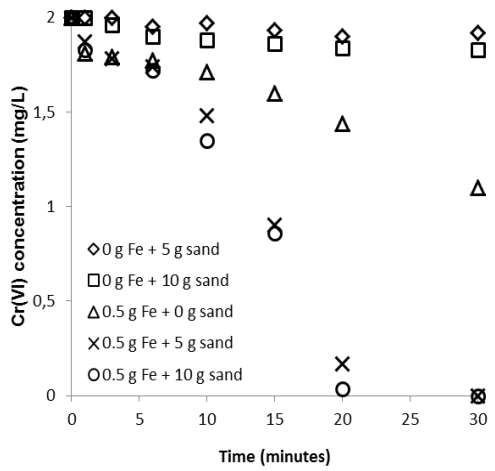

Fig.3. Cr(VI) vs. time for removal experiments with 0.5 g/L Fe^0 and two sand doses. For comparison purposes, control experiments with bare sand and bare Fe^0 are also plotted

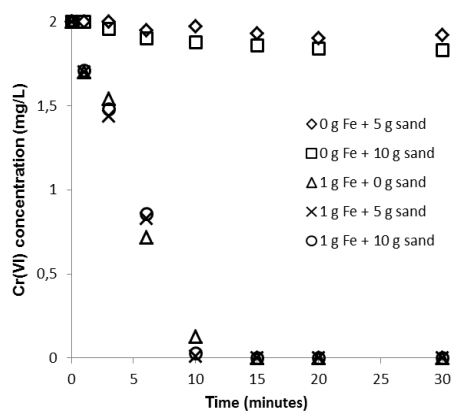

Fig.4. Cr(VI) vs. time for removal experiments with 1 g/L Fe^0 and two sand doses. For comparison purposes, control experiments with bare sand and bare Fe^0 are also plotted

In order to investigate the mechanism of Cr(VI) removal in H_2O-Fe^0-Cr(VI) system, the pH, Cr(VI), Cr(total), Fe(II) and Fe(total) concentrations were analyzed at the end of batch experiments with a 0.5 g/L Fe^0 dose, in the presence and absence of Cr(VI). It was observed that final Cr(total) concentration (1.9 mg/L) was lower than initial Cr(VI) concentration (2 mg/L) and greater than final Cr(VI) concentration (1.4 mg/L) (Fig.5B).

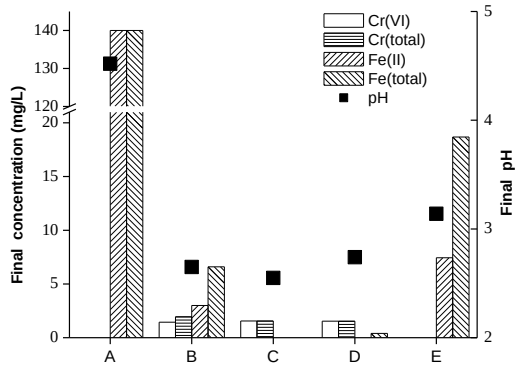

Fig.5. Profiles of final Cr(VI), Cr(total), Fe(II), Fe(total) and pH for Cr(VI) treatment with Fe^0 and MnO_2. A: 0.5 g Fe + 0.0 g MnO_2 + 0.0 mg Cr(VI); B: 0.5 g Fe + 0.0 g MnO_2 + 2.0 mg Cr(VI); C: 0.0 g Fe + 0.5 g MnO_2 + 2.0 mg Cr(VI); D: 0.5 g Fe + 0.5 g MnO_2 + 2.0 mg Cr(VI); E: 0.5 g Fe + 0.5 g MnO_2 + 0.0 mg Cr(VI)

This means that, from the 0.6 mg of Cr(VI) that disappeared from solution at the end of experiment, 0.5 mg (83.3%) were removed by reduction to Cr(III) and 0.1 mg (16.7%) by adsorption of $HCrO_4^-$ and/or adsorption/precipitation of Cr^{3+} on Fe^0 surface. However, since the final pH was 2.6, neither precipitation nor adsorption of Cr^{3+} can be considered plausible. Therefore, under the specific conditions involved in this study (initial pH 2.5, vigorous mixing, short-term duration), chemical reduction of Cr(VI) to Cr(III) was the main cause of Cr(VI) removal with metallic iron. This process may occur along two parallel pathways: 1) the heterogeneous reduction, involving electron transfer from Fe^0 surface (Eq.1) or from solid minerals containing Fe(II) formed onto the Fe^0 surface (Eq. 2-6); 2) the homogeneous reduction, occurring in the solution, in the presence of dissolved Fe^{2+} or H_2 (Eq. 7 and 8) generated during the heterogeneous reduction of Cr(VI) and Fe^0 corrosion (Eq. 9) (Gheju, 2011):

$$2HCrO_4^- + 3Fe^0 + 14H^+ \rightarrow 3Fe^{2+} + 2Cr^{3+} + 8H_2O \quad (1)$$

$$3FeCO_{3(s)} + HCrO_4^- + 8H_2O \rightarrow 4[Fe_{0,75}Cr_{0,25}](OH)_{3(S)} + 2H^+ + 3HCO_3^- \quad (2)$$

$$3[Fe^{II}_4Fe^{III}_2(OH)_{12}][SO_4 \cdot 3H_2O]_{(s)} + 4HCrO_4^- + 5H_2O \rightarrow 16[Fe_{0,75}Cr_{0,25}](OH)_{3(S)} + \\ + 2H^+ + 3SO_4^{2-} + 6Fe(OH)_{3(S)} \quad (3)$$

$$3Fe^{II}Fe^{III}_2O_{4(s)} + HCrO_4^- + 14H_2O + H^+ \rightarrow 4[Fe_{0,75}Cr_{0,25}](OH)_{3(S)} + 6Fe(OH)_{3(S)} \quad (4)$$

$$2FeS_{(s)} + 3CrO_4^{2-} + 9H_2O \rightarrow 4[Fe_{0,25}Cr_{0,75}](OH)_{3(S)} + Fe^{2+} + S_2O_3^{2-} + 6HO^- \quad (5)$$

$$3FeS_{2(s)} + CrO_4^{2-} + 8H^+ \rightarrow Cr^{3+} + 3Fe^{2+} + 3S_2^{2-} + 4H_2O \quad (6)$$

$$HCrO_4^- + 3Fe^{2+} + 7H^+ \rightarrow 3Fe^{3+} + Cr^{3+} + 4H_2O \quad (7)$$

$$1/3CrO_4^{2-} + 5/3H^+ + 1/2H_2 \rightarrow 1/3Cr^{3+} + 4/3H_2O \quad (8)$$

$$Fe^0 + 2H^+ \rightarrow Fe^{2+} + H_2 \quad (9)$$

By comparing the final parameters of the H_2O-Fe^0 and H_2O-Fe^0-Cr(VI) systems (Fig.5A şi B), it results that addition of Cr(VI) to H_2O-Fe^0 system led to a significant decrease of both pH and Fe(II)/Fe(total) concentrations. This suggests that oxidative dissolution of Fe^0 with H^+ (Eq.9), which is the sole process that consumes H^+ and generates Fe^{2+} in the H_2O-Fe^0 system, was markedly inhibited in the presence of Cr(VI). This phenomenon may be ascribed to a rapid adsorption of Cr(VI) onto Fe^0, process that blocks the access of H^+ to the Fe^0 surface. Subsequently, some of the adsorbed Cr(VI) could be reduced directly with Fe^0 (Eq.1). But, if the direct reduction with Fe^0 would have been the sole Cr(VI) reduction mechanism, and Eq. 9 would also have had a noticeable contribution to Fe^0 dissolution, then Fe(II) concentration should have been much greater than of Fe(III); normally, since at pH 2.6 both oxidation of Fe(II) to Fe(III) with dissolved O_2, and precipitation of Fe(III) are very slow, concentration of dissolved Fe(III) in the H_2O-Fe^0-Cr(VI) system should be close to zero at the end of a typical experiment. In fact, we noticed that Fe(II) and Fe(III) concentrations were about 45 and 65 %, respectively, from Fe(total) (Fig. 5B) which suggests that indirect reduction with dissolved Fe(II) was the major pathway of Cr(VI) reduction in H_2O-Fe^0-Cr(VI) system. This is consistent with recent research who support the view that Fe^0 should be regarded as generator of reducing agents, and contaminant reduction, when occurs, mainly results from indirect reducing agents generated due to Fe^0 corrosion (Noubactep, 2013). In order to describe the kinetic profile of Cr(VI) removal with Fe^0 under the experimental conditions tested here, three different mathematical models of chemical reactions were used: zero-order, first-order, and second-order (Coker, 2001). Based on regression analysis of kinetic data (Figs. 6-8), it was concluded that the process was best described by the zero-order model; this is in accord with several previous studies which have reported same kinetics with respect to the aqueous Cr(VI) concentration (Gheju, 2011). Experiments carried out to investigate the effect of temperature (Fig. 9) showed a favorable effect of increasing temperature on the efficiency of Cr(VI) removal, revealing an endothermic nature of the process; the results are in agreement with previous works, which reported a similar influence of temperature on Cr(VI) removal with Fe^0 (Gheju, 2011).

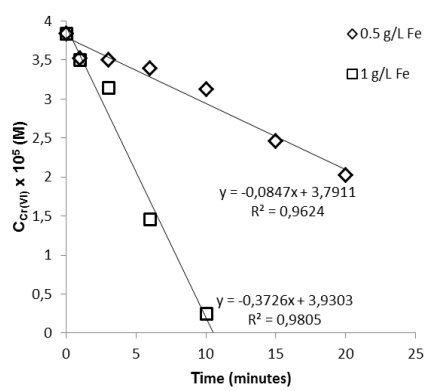

Fig.6. Linearized zero-order plots for Cr(VI) removal in H_2O-Fe^0-Cr(VI) system

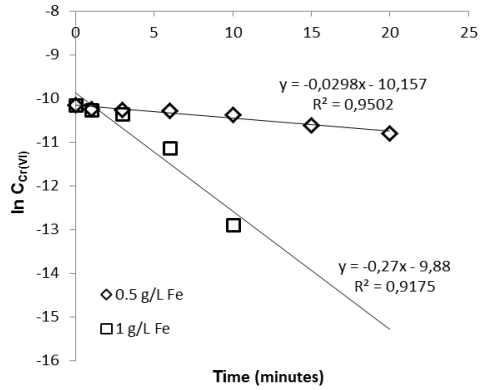

Fig.7. Linearized first-order plots for Cr(VI) removal in H_2O-Fe^0-Cr(VI) system

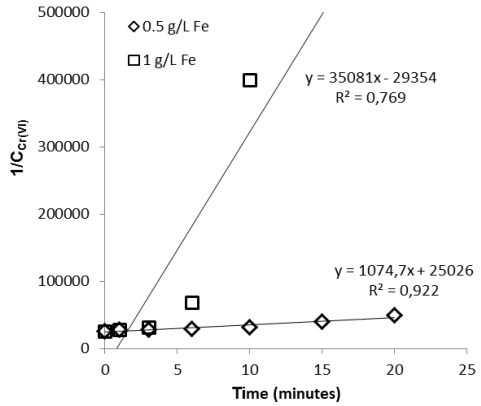

Fig.8. Linearized second-order plots for Cr(VI) removal in H_2O-Fe^0-Cr(VI) system

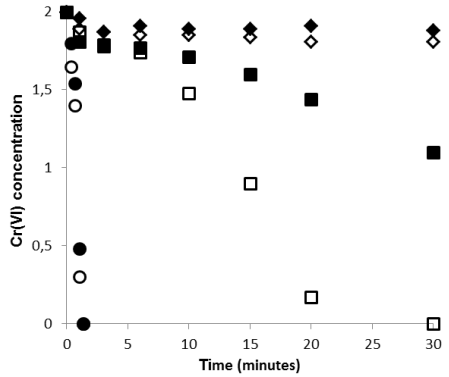

Fig.9. Effect of temperature on Cr(VI) removal in H_2O-Fe^0-Sand-Cr(VI) system. For comparison purposes, control experiments with bare Fe^0 are also plotted. ♦ 0.5 g Fe + 0 g sand, t = 6 ^oC; ■ 0.5 g Fe + 0 g sand, t = 22 ^oC; ● 0.5 g Fe + 0 g sand, t = 32 ^oC; ◊ 0.5 g Fe + 5 g sand, t = 6 ^oC; □ 0.5 g Fe + 5 g sand, t = 22 ^oC; ○ 0.5 g Fe + 5 g sand, t = 32 ^oC.

2.2.2. Removal of Cr(VI) in H_2O-Fe^0-Sand-Cr(VI) system

To address the effect of sand co-presence, batch experiments were conducted using Fe^0:sand mass ratios ranging from 1:5 to 1:20 (Fig.3 and 4). It is known that $HCrO_4^-$ anion can be retained on

mineral solids having hydroxyl groups on their surfaces, the efficiency of the adsorption process increasing with decreasing pH (Apte et al., 2006). In spite of the low pH involved in this study, only a minor loss of Cr(VI) (about 5% and 8%, at 5 g/L and 10 g/L sand, respectively) was noticed in experiments conducted in the presence of bare sand, over the time period of a typical experiment (Fig.3 and 4). In H_2O-Fe^0-Sand-Cr(VI) system, the effect of sand addition on Cr(VI) removal rate was highly dependent on the Fe^0 dose. At 0.5 g/L Fe^0, a noticeable favorable effect on Cr(VI) removal was observed, which, however, was only slightly influenced by the sand dose (Fig. 3). This positive effect can be attributed only to a very limited extent to sand ability to retain Cr(VI), or to sand capacity of reducing Fe^0 surface passivation by adsorbing the reaction products (Cr^{3+}, Fe^{2+}, Fe^{3+}), as previously suggested (Oh et al., 2007). The pH_{pzc} of sand found in this work was 7.3. This means that anions should be easily adsorbed at solution pH values less than 7.3, when sand surface will have positive mean surface charge density. However, in spite of the acidic conditions involved in this study, the efficiency of Cr(VI) adsorption on sand was low (Figs. 3 and 4). This is in accord with previous findings of Sharma et al. (2008) who noticed a Cr(VI) removal efficiency of about 12% over the same time period and at similar pH, but working with a Cr(VI) concentration and sand dose of 1.3 mg/L and 20 g/L, respectively. Instead, sorption of cations on mineral surface is detrimentally affected at more acidic pH (Bhargava et al., 2012), especially at pH values less than pH_{pzc}. Accordingly, several previous literature reports showed that efficiency of Cr(III) and Fe(II) adsorption on sand was low under acidic conditions, and increased only with increasing pH (Fendorf et al., 1994; Khamis et al., 2009; Sharma et al., 1999). Additionally, since the pH recorded at the end of batch experiments was generally slightly higher in the presence of sand than without sand (Fig. 10), the increase of Cr(VI) removal rate cannot be attributed neither to dissolution of sand and generation of protons, as previously suggested (Powell et al., 1995; Powell and Puls, 1997).

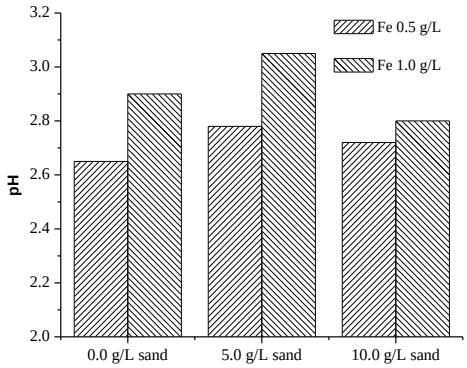

Fig.10. Profiles of final pH for Cr(VI) treatment with mixtures of Fe^0 and sand

Knowing that in H_2O-Fe^0-Cr(VI) unbuffered system the pH increases in time due to Fe^0 corrosion and Cr(VI) reduction (Gheju, 2011), the higher pH values observed at the end of sand-amended experiments could indicate that either Fe^0 corrosion, or Cr(VI) reduction, are favorably influenced by the co-presence of sand. It is hypothesized that the more rapid rates recorded for sand-amended experiments carried out at 0.5 g/L Fe^0 are the result of a synergistic effect between Cr(VI) adsorption on sand and a catalytic effect of sand on the reduction of adsorbed Cr(VI). Therefore, in addition to the mechanism presented in section 2.2.1, a third path of Cr(VI) removal can be hypothesized in the presence of sand, which may occur through the following steps (Eqs. 10-12): (1) generation of positively charged adsorption centers at the surface of sand, due to acidic conditions,

(2) Cr(VI) diffusion from the bulk solution to the sand surface, (3) adsorption of anionic Cr(VI) species on positively charged groups existent at sand surface, (4) reduction of adsorbed Cr(VI) with soluble Fe^{2+}, (5) desorption of reduction products (Cr^{3+}, Fe^{3+}) from sand surface due to electrostatic repulsion between the positively charged groups and the cations, and (6) transport of desorbed reduction products to the bulk solution

$$\equiv Si\text{-}OH + H^+ \Leftrightarrow \equiv Si\text{-}OH_2^+ \quad (10)$$

$$\equiv Si\text{-}OH_2^+ + HCrO_4^- \Leftrightarrow \equiv Si\text{-}OH_2^+HCrO_4^- \quad (11)$$

$$\equiv Si\text{-}OH_2^+HCrO_4^- + 3Fe^{2+} + 7H^+ \rightarrow \equiv Si\text{-}OH_2^+ + 3Fe^{3+} + Cr^{3+} + 4H_2O \quad (12)$$

The $\equiv Si\text{-}OH_2^+$ released in Eq.12 can then end up back in Eq.11, and thereby sustain the Cr(VI) reduction cycle. However, since the Cr(VI) adsorption capacity of sand is very low, the importance of this additional pathway seems to be highly dependent on the amount of soluble Fe^{2+} released in solution, thus, for a given pH, on Fe^0 dose. In contrast to experiments conducted at 0.5 g/L Fe^0 (Fig. 3), the favorable effect of sand was not observed at 1.0 g/L Fe^0 (Fig. 4). Therefore, it is apparent that contribution of heterogeneous reduction at sand surface to Cr(VI) removal in H_2O-Fe^0-Sand-Cr(VI) system is noticeable only at low Fe^0/Fe^{2+} concentrations, and decreases with increasing Fe^0 dose. The experimental results were kinetically evaluated using the same kinetic models applied for the control experiments with bare Fe^0 (Fig.11-16); it was shown that sand-assisted removal of Cr(VI) with Fe^0 fitted well to the zero-order kinetic model, at both 5.0 and 10.0 g/L sand doses.

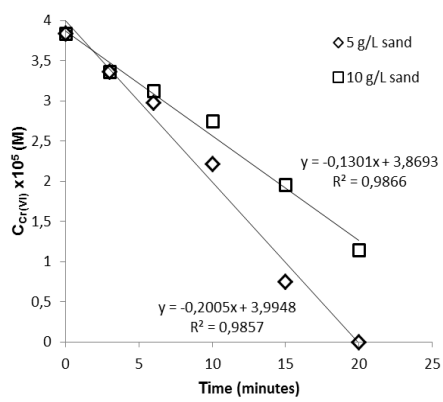

Fig.11. Linearized zero-order plots for Cr(VI) removal in H_2O-Fe^0-Sand-Cr(VI) system, at 0.5 g/L Fe^0

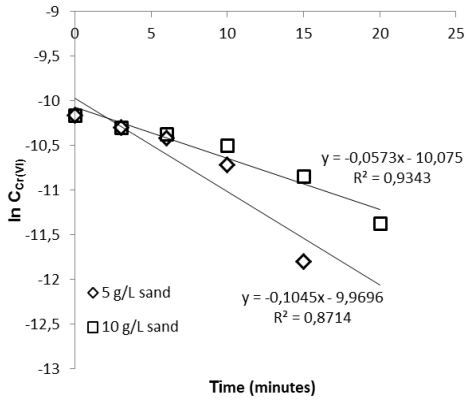

Fig.12. Linearized first-order plots for Cr(VI) removal in H_2O-Fe^0-Sand-Cr(VI) system, at 0.5 g/L Fe^0

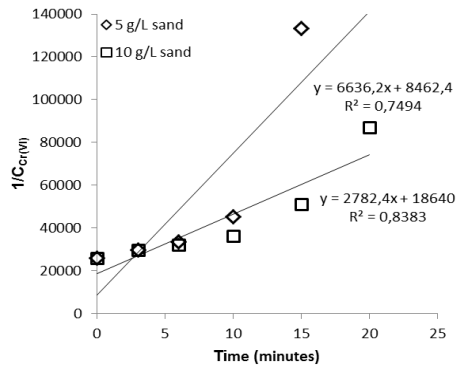

Fig.13. Linearized second-order plots for Cr(VI) removal in H_2O-Fe^0-Sand-Cr(VI) system, at 0.5 g/L Fe^0

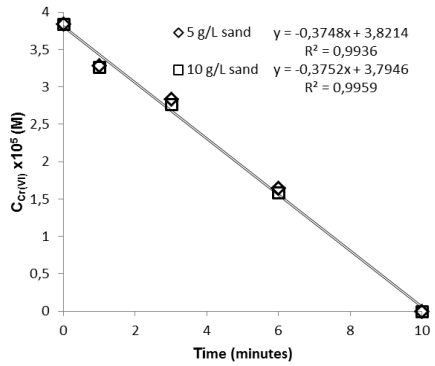

Fig.14. Linearized zero-order plots for Cr(VI) removal in H_2O-Fe^0-Sand-Cr(VI) system, at 1 g/L Fe^0

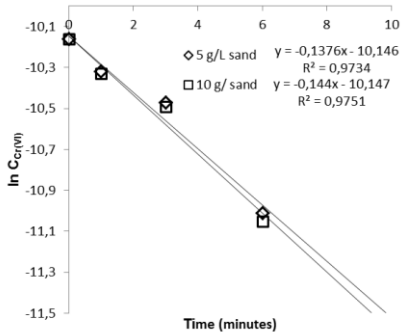

Fig.15. Linearized first-order plots for Cr(VI) removal in H_2O-Fe^0-Sand-Cr(VI) system, at 1 g/L Fe^0

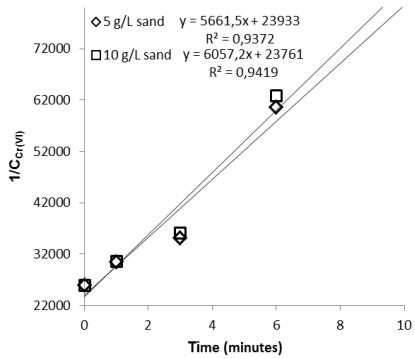

Fig.16. Linearized second-order plots for Cr(VI) removal in H_2O-Fe^0-Sand-Cr(VI) system, at 1 g/L Fe^0

Therefore, even though sand may have a favorable effect on the rate of Cr(VI) removal with low Fe^0 doses, the reaction order is not influenced by the presence of sand. Examining the effect of temperature on the removal of Cr(VI) in H_2O-Fe^0-Sand-Cr(VI) system (Fig.9), we observed a similar influence as for the H_2O-Fe^0-Cr(VI) system: rate of Cr(VI) removal increased with increasing temperature. This could be a confirmation of the fact that, in both systems (H_2O-Fe^0-Cr(VI) and H_2O-Fe^0-Sand-Cr(VI)) the main mechanism responsible for the removal of Cr(VI) was chemical reduction of Cr(VI) with Fe(II).

In order to investigate the influence of the sand size on the efficiency of Cr(VI) removal with Fe^0, 1000 mL Cr(VI) solution 2 mg/L with pH 2.5 were reacted with 30 g sand with following sizes: 0.1-0.5 mm, 0.5-1.25 mm, 1.25-2 mm, and 2-5 mm. The results (Fig.17), indicate the fact that the co-presnce of sand has a favorable effect on Cr(VI) removal with Fe^0.

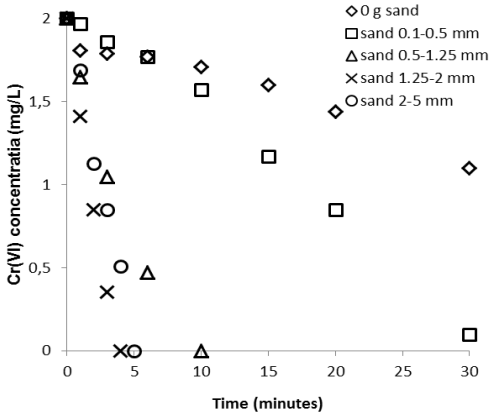

Fig.17. Cr(VI) vs. time for removal experiments with 0.5 g/L Fe^0 and 30 g/L sand, as a function of sand size. For comparison purposes, control experiments with bare bare Fe^0 are also plotted

It was noticed that by increasing the size of sand from 0.1-0.5 mm to 1.25-2 mm, the efficiency of Cr(VI) removal with Fe^0 also increases; however, a further increase of the size of sand to 2-5 mm was followed by a slight decrease in the efficiency of Cr(VI) removal. This was confirmed also by the analysis of the final pH values and final Fe(total) concentrations, presented in Figs.18 and 19. It can be seen that both final pH values and final Fe(total) concentrations are increasing with increasing sand size, having the highest value for the sand with 1.25-2 mm. Higher pH values and final Fe(total) concentrations means that both the indirect reduction of Cr(VI) with Fe(II) and the oxidative dissolution of Fe^0 were favored.

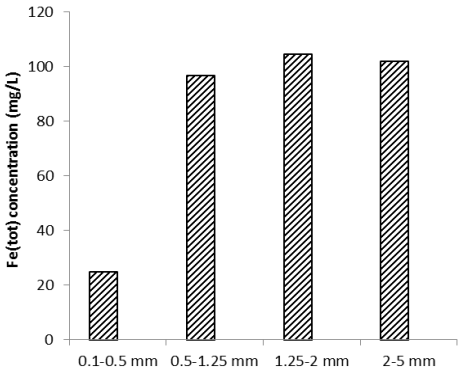

Fig.18. Profiles of final Fe(total) in the H_2O-Fe^0-Sand-Cr(VI) system, as a function of sand size

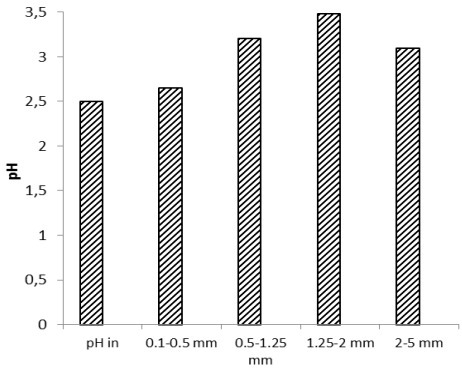

Fig.19. Profiles of final pH in the H_2O-Fe^0-Sand-Cr(VI) system, as a function of sand size.

2.3. Conclusions

Experiments carried out in H_2O-Fe^0-Cr(VI) system indicated that chemical reduction with Fe(II) was the main cause of Cr(VI) removal, and that reaction order was zero with respect to Cr(VI). Temperature had a positive influence on Cr(VI) removal with Fe^0: while at 6 ^oC the process was quasi-inhibited, its efficiency significantly increased with increasing temperature up to 32 ^oC. The co-presence of sand induced a positive effect on Cr(VI) removal with Fe^0, but only at low Fe^0 doses; this phenomenon was ascribed to a catalytic effect of sand on reduction of Cr(VI) adsorbed on sand. The efficiency of Cr(VI) removal with Fe^0 decreased in following order: 1.25-2 mm > 2-5 mm > 0.5-1.25 mm >> 0.1-0.5 mm. The main mechanism contributing to Cr(VI) removal in H_2O-Fe^0-Sand-Cr(VI) system was chemical reduction with Fe(II), regardless of the sand dose. Both in presence and absence of sand, Cr(VI) removal with Fe^0 followed a zero-order kinetics, being favored by an increase of temperature over the range of 6-32 ^oC.

Objective 2. Investigation of the effect of MnO_2 co-presence on Cr(VI) removal with Fe^0

Activities: Batch treatability experiments for Cr(VI) removal with Fe^0 in the co-presence of MnO_2

3.1. Materials and methods

Commercially available MnO_2 (pyrolusite ≥ 90%, ~10 μm) and Fe^0 (≥ 99%, ~10 μm), both from Merck, were used in this study as received. The experimental and analytical methods were the same as those described at section 2.1.

3.2. Results and discussion

Removal of Cr(VI) in H_2O-Fe^0-MnO_2-Cr(VI) system

To address the effect of MnO_2 co-presence, batch experiments were conducted using Fe^0:MnO_2 mass ratios ranging from 1:0.5 to 1:2. The results (Fig.20) have shown that the removal process proceeds in two stages: rapid removal rates are observed within the first time interval (first 3 minutes), followed by a sharp rate decline and cessation of the reaction in the second one; the higher the MnO_2 dose, the faster the removal rate of Cr(VI), regardless of the Fe^0 dose.

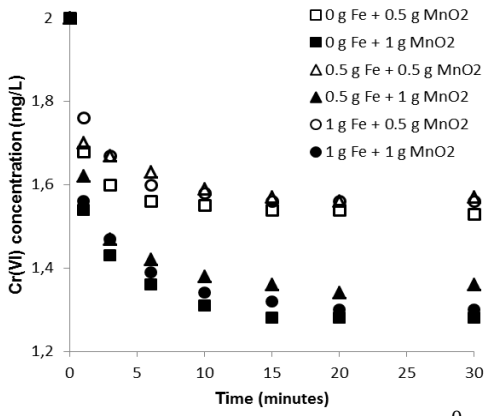

Fig.20. Cr(VI) vs. time for removal experiments with different Fe^0 and MnO_2 mixtures. For comparison purposes, control experiments with bare MnO_2 are also plotted

In contrast with the H_2O-Fe^0-Cr(VI) system (Fig.5B) where a 0.5 mg/L Cr(III) concentration was detected, no Cr(III) was identified in H_2O-Fe^0-MnO_2-Cr(VI) system (Fig.5D) at the end of experiment. Due to acidic conditions involved in this study, the total absence of Cr(III) cannot be attributed to precipitation or adsorption processes involving Cr(III). Hence, the total absence of Cr(III) in H_2O-Fe^0-MnO_2-Cr(VI) system can be ascribed to one of the following two causes: 1) Cr(VI) was not at all reduced, and adsorption on MnO_2 was the sole removal mechanism for Cr(VI), and 2) Cr(VI) was mainly adsorbed on MnO_2 and also reduced to some extent, but the entire amount of Cr(III) that resulted was subsequently rapidly re-oxidized with MnO_2. MnO_2 is known as an effective oxidant of Cr(III), especially at low pH (Chung and Zasoski, 2002; Fendorf, 1995; Landrot et al., 2010):

$$Cr^{3+} + H_2O + 1.5MnO_2 \rightarrow HCrO_4^- + 1.5Mn^{2+} + H^+ \quad (13)$$

In order to investigate the oxidative capacity of MnO_2 towards Cr(III) under the specific conditions of this study, 1000 mL solution 2 mg/L Cr(III) were reacted with 0.5 g MnO_2 at pH 2.5. The results (Fig.21) show that oxidation of Cr(III) was very rapid.

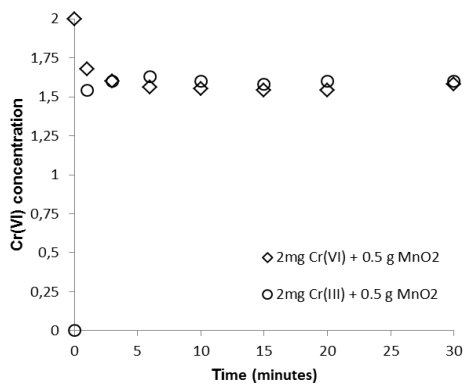

Fig.21. Comparison of Cr(VI) depletion in H_2O-MnO_2-Cr(VI) system with the generation of Cr(VI) in H_2O-MnO_2-Cr(III) system

However, the final concentration of Cr(VI) was lower than initial concentration of Cr(III) (1.6 vs 2 mg/L), indicating that Cr(VI) was partially retained on MnO_2, process favored by the acidic pH. The amount of Cr(VI) adsorbed after Cr(III) oxidation with MnO_2 was very close to the amount of Cr(VI) adsorbed at equilibrium in H_2O-MnO_2-Cr(VI) system (~ 0.4 mg, Fig.21). Hence, the maximum adsorption capacity of MnO_2 at a 0.5 g/L dose was approximately 0.8 mg/g. If reduction of Cr(VI) would be the main removal pathway in H_2O-Fe^0-MnO_2-Cr(VI) system, the decrease of Cr(VI) concentration should occur slower than in H_2O-Fe^0-Cr(VI) system, as a result of the constant and rapid re-oxidation of Cr(III). But, in fact, it was noticed that disappearance of Cr(VI) in H_2O-Fe^0-MnO_2-Cr(VI) system was actually faster than in H_2O-Fe^0-Cr(VI) system, at least for the first 15 minutes (Fig.22).

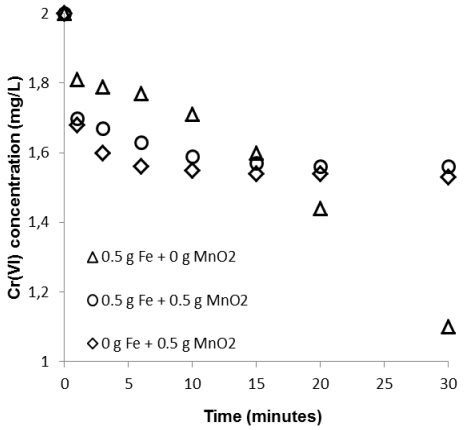

Fig.22. Comparison of Cr(VI) depletion in H_2O-Fe^0-MnO_2-Cr(VI), H_2O-MnO_2-Cr(VI) and H_2O-Fe^0-Cr(VI) system

On the other hand, if adsorption of Cr(VI) on MnO_2 would be the main removal pathway in H_2O-Fe^0-MnO_2-Cr(VI) system and reduction to Cr(III) only a possible minor route, the decrease of Cr(VI) concentration should occur slower than in H_2O-MnO_2-Cr(VI) system, also as a result of the constant and rapid re-oxidation of Cr(III). Fig.22 confirm this last hypothesis, suggesting that total absence of Cr(III) in H_2O-Fe^0-MnO_2-Cr(VI) may be explained by the predominance of the adsorption mechanism, while the reduction mechanism, if occurred, was negligible.

To obtain further evidences on the removal mechanism of Cr(VI) in H_2O-Fe^0-MnO_2-Cr(VI) system, the speciation of Fe was also analyzed at the end of experiments. Just like Cr(III), Fe(II) was also not detected in H_2O-Fe^0-MnO_2-Cr(VI) system (Fig.5D); moreover, Fe(total) concentration was 16.5 times lower than in H_2O-Fe^0-Cr(VI) system (6,6 mg/L, Fig.5B). Instead, Fe(II)/Fe(total) concentrations in H_2O-Fe^0-MnO_2 system were much higher than in H_2O-Fe^0-MnO_2-Cr(VI) system, and much lower than in H_2O-Fe^0 system (Fig.5A). A significant decrease (86.6%) of Fe(total) concentration, coupled with the presence of Fe(III), was observed at the end of experiment in H_2O-Fe^0-MnO_2 system, compared to H_2O-Fe^0 system. An even more notable decrease (99.7%) of Fe(total) concentration, coupled with the absence of Fe(II), was observed at the end of experiment in H_2O-Fe^0-MnO_2-Cr(VI) system, compared to H_2O-Fe^0 system. Due to acidic conditions (final pH 2.7-3.1), it is obvious that precipitation of soluble Fe species cannot be responsible for this phenomenon. It is known that oxidation of Fe(II) by MnO_2 (Eq. 14) is very fast under acidic conditions (Han et al., 2011):

$$2Fe^{2+} + MnO_2 + 4H^+ \rightarrow 2Fe^{3+} + Mn^{2+} + 2H_2O \qquad (14)$$

In order to investigate whether adsorption of soluble Fe species on MnO_2, followed by oxidation of Fe(II), was the cause of Fe(II) absence and Fe(total) decrease in H_2O-Fe^0-MnO_2-Cr(VI) system, 0.5 g MnO_2 were reacted with 1000 mL solution 140 mg/L Fe(II), at pH 2.5.

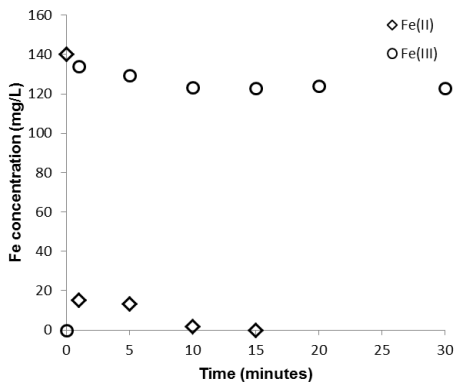

Fig.23. Comparison of Fe(II) depletion and Fe(III) generation in H_2O-MnO_2-Fe(II) system

Fig.23 shows that oxidation of Fe(II) was very fast, being complete after about 10 minutes, which could explain the absence of Fe(II) in H_2O-Fe^0-MnO_2-Cr(VI) system. However, the decrease of Fe(total) concentration at the end of this control experiment was only 12.1%, attributable to adsorption processes on MnO_2 which, in this work, was found to have a pH_{pzc} value of 5.8. Therefore, adsorption of soluble Fe species on MnO_2 can also not justify the significant decrease of Fe(total) in H_2O-Fe^0-MnO_2 and H_2O-Fe^0-MnO_2-Cr(VI) systems. The only explanation that remains is that Fe^0 corrosion by H^+ (Eq. 9), which is responsible for the generation of important Fe(total) concentrations in H_2O-Fe^0 system (Fe(total) = 140 mg/L), was severely inhibited as a result of MnO_2 co-presence in H_2O-Fe^0-MnO_2 system (Fe(total) = 18.6 mg/L) and in H_2O-Fe^0-MnO_2-Cr(VI) system (Fe(total) = 0.4 mg/L). Therefore, addition of MnO_2 inhibits generation of Fe(II) in H_2O-Fe^0-MnO_2-Cr(VI) system, obstructing thus indirect reduction of Cr(VI) by Fe(II) (Eq.7). Since Fe^0 oxidation by H^+ was detrimentally affected by the presence of MnO_2, it is highly probable that Fe^0 oxidation by Cr(VI) (Eq.1) was similarly influenced. Furthermore, it can be seen that, at same MnO_2 dose, Cr(VI) removal efficiency (Figs. 5C and 5D, supplementary material) and Cr(VI) removal pattern (Fig. 20) in H_2O-MnO_2-Cr(VI) and H_2O-Fe^0-MnO_2-Cr(VI) systems are almost similar.

Summarizing, both Fe and Cr speciation analysis suggest that, due to co-presence of MnO_2, adsorption on MnO_2 and not chemical reduction with Fe^0/Fe(II) was the main mechanism responsible for Cr(VI) removal in H_2O-Fe^0-MnO_2-Cr(VI) system. This is in accord with previous studies which have reported that manganese oxides are strong adsorbents for metallic ions (Postma and Appelo, 2000, Wang et al., 2013). Once established the mechanism, the next question that arises is: why was corrosion of Fe^0 hindered in the presence of MnO_2? Since the size of MnO_2 and Fe^0 particles was comparable, but their density was 5.03 g/cm^3 (MnO_2) and 7.87 g/cm^3 (Fe^0), the volume (and therefore, the specific surface area) of a given amount of solid (i.e., 0.5 g) was much greater for MnO_2 than for Fe^0. Accordingly, it was hypothesized that, due to the vigorous mixing and differences in surface electrical charge (pH_{pzc} 8.3 for Fe^0 (Sun et al., 2006) and 5.8 for MnO_2), MnO_2 particles were attached to the surface of Fe^0 particles, inhibiting thus reactions 1 and 9 by blocking the access of $HCrO_4^-$ and H^+ ions to the Fe^0 surface. Hence, the Fe^0 surface alteration induced by MnO_2 appears to be the cause of Cr(VI) reduction inhibition in H_2O-Fe^0-MnO_2-Cr(VI) system, determining adsorption on MnO_2 to be the main mechanism responsible for the removal of Cr(VI).

By investigating the effect of temperature on Cr(VI) removal in H_2O-Fe^0-MnO_2-Cr(VI) system (Fig.24), we noticed a slight decrease in Cr(VI) removal rate as the temperature increased from 6 ^oC to 22 ^oC, followed by a sharp increase when temperature was further raised to 32 ^oC.

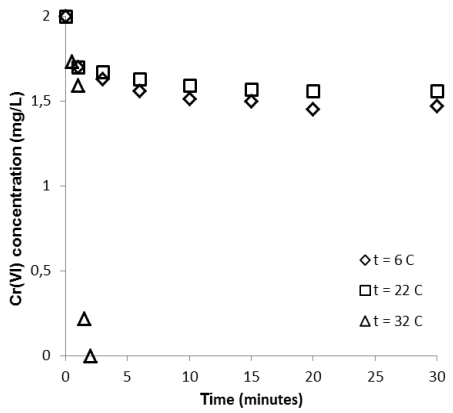

Fig.24. Effect of temperature on Cr(VI) removal in H_2O-Fe^0-MnO_2-Cr(VI) system, at 0.5 g/L Fe^0 and 0.5 g/L MnO_2

The results at 6 and 22 ^oC are in agreement with previous reports who indicated that Cr(VI) adsorption on MnO_2 systems is detrimentally affected by the increase of temperature (Bhutani et al., 1992). Since Cr(VI) removal in H_2O-Fe^0-Cr(VI) system was almost totally inhibited at 6 ^oC (Fig.9), it is obvious that adsorption was the main mechanism responsible for Cr(VI) removal in H_2O-Fe^0-MnO_2-Cr(VI) system not only at 22 ^oC, but also at 6 ^oC. Instead, the results obtained at 32 ^oC suggest that, at this temperature, the disappearance of Cr(VI) was the result of a different mechanism than at 6 and 22 ^oC. If the removal mechanism would have been the same (i.e. adsorption on MnO_2) over the entire temperature range, than Cr(VI) removal rates in H_2O-Fe^0-MnO_2-Cr(VI) system should decrease in the following order: 6 ^oC > 22 ^oC > 32 ^oC. Instead, the fastest Cr(VI) removal was observed at 32 ^oC, being complete after about 2 minutes (Fig. 24). This behavior is very similar to removal of Cr(VI) in H_2O-Fe^0-Cr(VI) system at 32 ^oC (Fig. 9), when chemical reduction with Fe(II) was the main mechanism. In order to achieve a better understanding of the temperature influence, the pH, Fe(II) and Fe(total) concentrations measured at the end of experiments conducted at 22 ^oC and 32 ^oC were summarized in Fig. 25 and further analyzed.

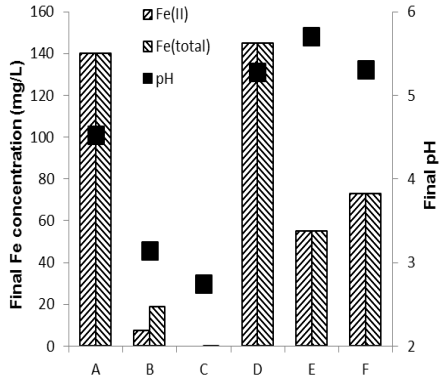

Fig.25. Profiles of final Fe(II), Fe(total) and pH for experiments at 22 and 32 ^oC. A: 0.5 g Fe + 0 g MnO_2 + 0 mg Cr(VI), t = 22 ^oC; B: 0.5 g Fe + 0.5 g MnO_2 + 0 mg Cr(VI), t = 22 ^oC; C: 0.5 g Fe + 0.5 g MnO_2 + 2 mg Cr(VI), t = 22 ^oC; D: 0.5 g Fe + 0 g MnO_2 + 0 mg Cr(VI), t = 32 ^oC; E: 0.5 g Fe + 0.5 g MnO_2 + 0 mg Cr(VI), t =32 ^oC; F: 0.5 g Fe + 0.5 g MnO_2 + 2 mg Cr(VI), t = 32 ^oC

Fig. 25 shows that the increase of temperature from 22 ^{o}C to 32 ^{o}C was not followed by an important enhancement of Fe^0 dissolution in H_2O-Fe^0 system (Fig. 25A and 25D); instead, a significant enhancement of Fe^0 dissolution was observed in H_2O-Fe^0-MnO_2 (Fig. 25B and 25E) and H_2O-Fe^0-MnO_2-Cr(VI) (Fig. 25C and 25F) systems, leading to much higher amounts of dissolved Fe(II) at 32 ^{o}C than at 22 ^{o}C. These notable differences indicate that, while at 22 ^{o}C MnO_2 has a deleterious effect on Fe^0 corrosion, at 32 ^{o}C the co-presence of MnO_2 exerts a positive influence. Thus, at 32 ^{o}C, reduction of Cr(VI) with Fe(II) seems to be the main removal mechanism of Cr(VI) in H_2O-Fe^0-MnO_2-Cr(VI) system, just like in H_2O-Fe^0-Cr(VI) system. No Cr(III) was identified in the solution at the end of experiments at 32 ^{o}C. The absence of Cr(III) may be attributed to its precipitation and/or adsorption on MnO_2 and Fe^0, both processes being favored by the increase of pH up to 5.3 (Fig.25). Similarly, the absence of a low Fe(III) concentration (~ 6.5 mg/L) that should theoretically exist in solution as a result of Cr(VI) indirect reduction, may be ascribed to precipitation and/or adsorption processes.

Because it was established that adsorption was the main mechanism governing removal of Cr(VI) in H_2O-Fe^0-MnO_2-Cr(VI) system at 22 ^{o}C, the experimental data was further analyzed from kinetic standpoint by applying two models commonly used in sorption processes: the pseudo first and pseudo second-order equations (S.S. Gupta and Bhattacharyya, 2011; Ho, 2006); the results showed that removal of Cr(VI) in H_2O-Fe^0-MnO_2-Cr(VI) system obeys the pseudo second-order kinetic model, which provides the best regression analysis results; moreover, this model also produced the best match between the predicted and the experimental determined values of equilibrium adsorption capacities (Figs. 26-29).

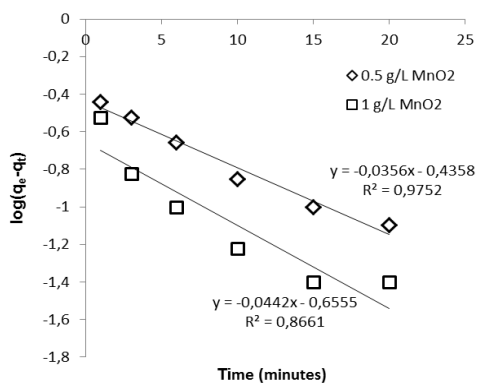

Fig.26. Linearized pseudo first-order plots for Cr(VI) removal in H_2O-Fe^0-MnO_2-Cr(VI) system, at 0.5 g/L Fe^0 and two different MnO_2 doses

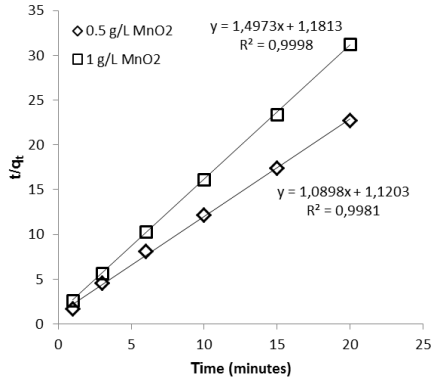

Fig.27. Linearized pseudo second-order plots for Cr(VI) removal in H_2O-Fe^0-MnO_2-Cr(VI) system, at 0.5 g/L Fe^0 and two different MnO_2 doses

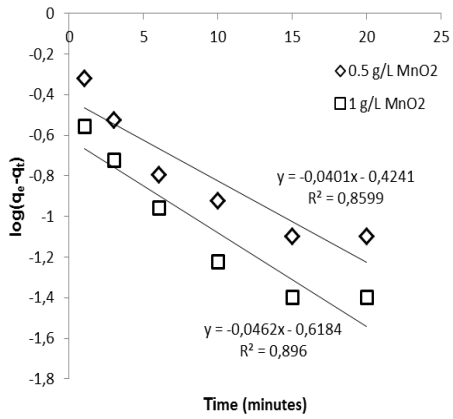

Fig.28. Linearized pseudo first-order plots for Cr(VI) removal in H_2O-Fe^0-MnO_2-Cr(VI) system, at 1 g/L Fe^0 and two different MnO_2 doses

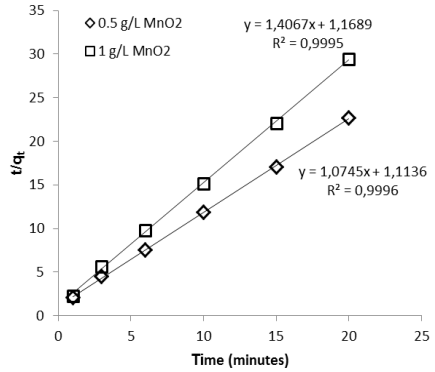

Fig.29. Linearized pseudo second-order plots for Cr(VI) removal in H_2O-Fe^0-MnO_2-Cr(VI) system, at 1 g/L Fe^0 and two different MnO_2 doses

3.3. Conclusions

In contrast to the H_2O-Fe^0-Cr(VI) and H_2O-Fe^0-Sand-Cr(VI) systems, in H_2O-Fe^0-MnO_2-Cr(VI) system the major removal mechanism seems to be adsorption on MnO_2, which obeys the pseudo second-order kinetic model. It was also demonstrated that oxidative dissolution of Fe^0 was significantly inhibited in the presence of MnO_2. The removal rates in H_2O-Fe^0-MnO_2-Cr(VI) system

decreased in the following order: 32 ^{o}C >> 6 ^{o}C > 22 ^{o}C. This temperature dependence suggest that, at 32 ^{o}C, the detrimental effect of MnO_2 on Fe^0 corrosion was annihilated, leading to generation of an important amount of Fe(II), which subsequently reduced very rapidly Cr(VI). Therefore, in spite of the MnO_2 co-presence, the major Cr(VI) removal mechanism at 32 ^{o}C in H_2O-Fe^0-MnO_2-Cr(VI) system was the indirect chemical reduction of Cr(VI) to Cr(III) with Fe(II).

Objective 4. Dissemination of the obtained results
Activities: Analysis and interpretation of experimental data. Writing of scientific articles.

Scientific papers were written and submitted to journals and international conferences.

Objective 5. Self-evaluation of the project
Activities: The degree of achievement of objectives for the 2015 stage was analyzed. It was concluded that all the proposed objectives were fully achieved, so there was no need to make any corrective action.

References

APHA, AWWA, WEF, 1995. Standard methods for the examination of water and wastewater, 19th edition. United Book Press, Inc., Baltimore.

Apte A.D., Tare V., Bose P., 2006. Extent of oxidation of Cr(III) to Cr(VI) under various conditions pertaining to natural environment. J. Hazard. Mater. B128, 164-174.

Bhargava, A., Carmona, F.F., Bhargava, M., Srivastava, S., 2012. Approaches for enhanced phytoextraction of heavy metals. J. Environ. Manag. 105, 103-120.

Bhutani, M.M., Mitra, A.K., Kumari, R., 1992. Kinetic study of Cr(VI) sorption on MnO_2, J. Radioanal. Nucl. Ch. 157(1), 75-86.

Chung, J.B., Zasoski, R.J., 2002. Oxidation of Cr(III) to Cr(VI) by pyrolusite. Agric. Chem. Biotechnol. 45(3), 125-130.

Coker, A.K., 2001. Modeling of chemical kinetics and reactor design. Gulf Professional Publishing, Houston.

Eary, L.E., Rai, D., 1987. Kinetics of chromium(III) oxidation to chromium(VI) by reaction with manganese dioxide. Environ. Sci. Technol. 21, 1187-1193.

Fendorf, S.E., Lamble, G.M., Stapleton, M.G., Kelley, M.J., Sparks, D.L., 1994. Mechanisms of chromium(III) sorption on silica. 1. Cr(III) surface structure derived by extended x-ray absorption fine structure spectroscopy. Environ. Sci. Technol. 28, 204-289.

Fendorf, S.E., 1995. Surface reactions of chromium in soil and waters. Geoderma 67, 55-71.

M. Gheju, A. Iovi, Kinetics of hexavalent chromium reduction by scrap iron, J. Hazard. Mater., B135 (1-3), 2006, 66-73.

Gheju, M., 2011. Hexavalent chromium reduction with zero-valent iron (ZVI) in aquatic systems. Water Air Soil Pollut. 222(1-4), 103-148.

Gupta, S.S., Bhattacharyya, K.G., 2011. Kinetics of adsorption of metal ions on inorganic materials: a review. Adv. Colloid Interface Sci. 162, 39-58.

Khamis, M., Jumean, F., Abdo, N., 2009. Speciation and removal of chromium from aqueous solution by white, yellow and red UAE sand. J. Hazard. Mater. 169, 948-952.

Han, X., Li, Y.L., Gu, J.D., 2011. Oxidation of As(III) by MnO_2 in the absence and presence of Fe(II) under acidic conditions. Geochim. Cosmochim. Acta 75, 368-379.

Ho, Y.S., 2006. Review of second-order models for adsorption systems. J. Hazard. Mater. B136, 681-689.

Landrot, G, Ginder-Vogel, M., Sparks, D.L., 2010. Kinetics of chromium(III) oxidation by manganese(IV) oxides using quick Scanning X-ray Absorption Fine Structure Spectroscopy (Q-XAFS). Environ. Sci. Technol. 44(1), 143-149.

Noubactep, C., 2013. Metallic iron for water treatment: a critical review. Clean - Soil Air Water 41(7), 702-710.

Oh, Y.J., Song, H., Shin, W.S., Choi, S.J., Kim, Y.H., 2007. Effect of amorphous silica and silica sand on removal of chromium(VI) by zero-valent iron. Chemosphere 66, 858-865.

Postma, D., Appelo, C.A.J., 2000. Reduction of Mn-oxides by ferrous iron in a flow system: column experiment and reactive transport modeling. Geochim. Cosmochim. Acta 64(7), 1237-1247.

Powell, R.M., Puls, R.W., Hightower, S.K., Sabatini, D.A., 1995. Coupled iron corrosion and chromate reduction: mechanisms for subsurface remediation. Environ. Sci. Technol. 29, 1913-1922.

Powell, R.M., Puls, R.W., 1997. Proton generation by dissolution of intrinsic or augmented aluminosilicate minerals for in situ contaminant remediation by zero-valence-state iron. Environ. Sci. Technol. 31, 2244-2251.

Sharma, S.K., Greetham, M.R., Schippers, J.C., 1999. Adsorption of iron(II) onto filter media. J. Water Supply Res. T. 48(3), 84-91.

Sun, Y.P., Li, X.Q., Cao, J., Zhang, W.X., Wang, H.P., 2006. Characterization of zero-valent iron nanoparticles. Adv. Coll. Interf. Sci. 120, 47-56

Wang, Z., Lee, S.W., Catalano, J.G., Lezama-Pacheco, J.S., Bargar, J.R., Tebo, B.M., Giammar, D.E., 2013. Adsorption of uranium(VI) to manganese oxides: X-ray absorption spectroscopy and surface complexation modeling. Environ. Sci. Technol. 47, 850-858.

Zach-Maor, A., Semiat, R., Shemer, H., 2011. Synthesis, performance, and modeling of immobilized nano-sized magnetite layer for phosphate removal. J. Colloid Interf. Sci. 357, 440-446.